

Review and experimental analysis of oxidative torrefaction of sugarcane bagasse, sawdust, and rice husk in concrete

Saranya Nithiyandan¹✉, Ramaiah Prakash², Vadivelu Navin Ganesh³, Shenbagaraman Panneerselvam¹, Saraswathi Radhakrishnan¹ and Manoj Prabhakar⁴

¹ Coimbatore Institute of Technology, Department of Civil Engineering, Coimbatore, Tamil Nadu, India

² Alagappa Chettiar Government College of Engineering and Technology, Department of Civil Engineering, Karaikudi, Tamil Nadu, India

³ PSG Institute of Technology and Applied Research, Department of Civil Engineering, Coimbatore, Tamil Nadu, India

⁴ National Institute of Technology, Department of Energy and Environment, Tiruchirappalli, Tamil Nadu, India

Corresponding author:
Saranya Nithiyandan

Received:
September 2, 2025

Revised:
February 11, 2026

Accepted:
February 25, 2026

Published:
June 11, 2026

Citation:
Nithiyandan, S. et al.
Review and experimental analysis of oxidative torrefaction of sugarcane bagasse, sawdust, and rice husk in concrete.
Advances in Civil and Architectural Engineering, 2026, 17 (32), pp. 170-188.
<https://doi.org/10.13167/2026.32.10>

ADVANCES IN CIVIL AND ARCHITECTURAL ENGINEERING
(ISSN 2975-3848)

Faculty of Civil Engineering and Architecture Osijek
Josip Juraj Strossmayer University of Osijek
Vladimira Preloga 3
31000 Osijek
CROATIA



Abstract:

The growing global emphasis on sustainable, low-carbon energy has intensified interest in biomass as a renewable substitute for fossil fuels, with torrefaction emerging as an effective thermal pretreatment for enhancing fuel properties, particularly for co-firing in coal-based power plants. This study examines the oxidative torrefaction of three widely available lignocellulosic residues sugarcane bagasse, sawdust, and rice husk processed at 200, 250, and 300 °C for 30 min under ambient air conditions to simulate oxidative environments. Fuel quality improvements and physicochemical transformations were assessed using proximate analysis, calorific value measurements, energy dispersive X-ray spectroscopy, Fourier transform infrared spectroscopy, and thermogravimetric analysis. The results indicate that oxidative torrefaction significantly enhances biomass characteristics by increasing fixed carbon content, reducing moisture and volatile matter, and improving calorific value. Among the materials studied, sawdust exhibited the most pronounced enhancement, attaining a calorific value of 5941,53 kcal/kg and the highest carbon concentration, followed by sugarcane bagasse, while rice husk showed moderate improvement due to its higher ash and silica content. Overall, the findings demonstrate the suitability of torrefied biomass for integration into existing coal-fired systems, supporting emission reduction, cleaner energy generation, and alignment with India's energy transition and carbon mitigation objectives.

Keywords:

biomass; co-firing; rice husk; sawdust; sugarcane bagasse

1 Introduction

Globally, coal has long supported electricity generation; however, sustainability concerns have pushed many economies towards alternatives [1; 2]. The EU enforces strict biomass sustainability criteria under the Renewable Energy Directive III (2023). The UK has almost entirely converted plants such as Drax to biomass. Japan relies on biomass imports, particularly wood pellets and palm kernel shells, through its Feed-in Tariff program, and is piloting ammonia co-firing. In North America, biomass trials in pulverised coal and fluidised bed boilers are shaped by renewable portfolio standards and state-level carbon policies [3-6]. Collectively, these efforts show a global shift to co-firing and biomass substitution as pathways to balance energy security with emission reduction. To contextualise these transitions, Figure 1 presents the global primary energy demand distribution, highlighting the relative shares of coal, oil, natural gas, nuclear energy, and renewables.

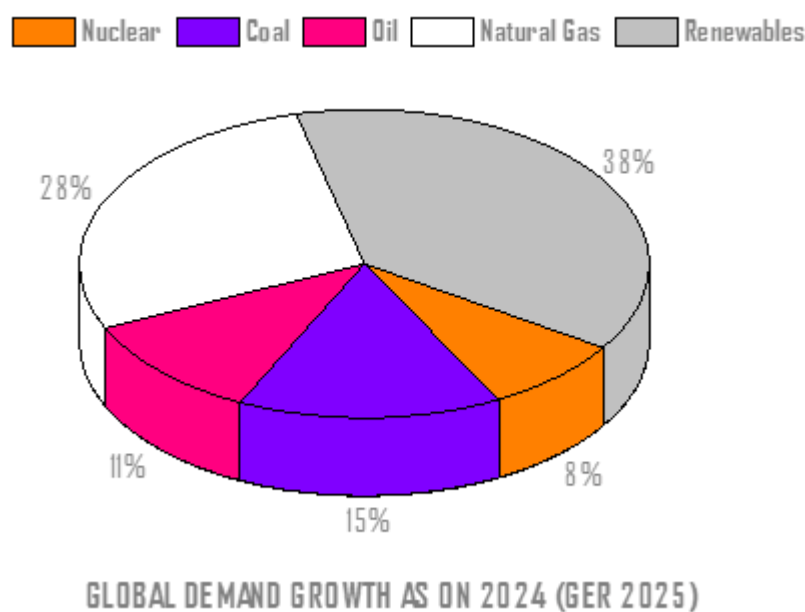


Figure 1. Global demand growth [5]

India has followed a similar trajectory. Coal still accounts for more than 70 % of the national power production, with the 2018 energy mix comprising coal (46 %), crude oil (29,6 %), natural gas (6,2 %), hydro (3,9 %), nuclear (1,1 %), and renewable energy (3,4 %) [7]. To address environmental challenges, India mandated biomass co-firing in October 2022, starting with 5 % blending and increasing it to 7 %. This policy can utilise over 700 million tonnes of crop residues annually, reducing stubble burning and associated pollution. Despite abundant reserves 361,41 billion tonnes as of April 2022, with 52 % proven in Odisha, Jharkhand, and Chhattisgarh [8; 9], the effective utilization of these resources remains constrained. The country is accelerating renewable energy and biomass integration [10-12]. Infrastructure upgrades such as 214 million tonnes of coal washery capacity per year and 23 operating refineries further strengthen this sector [9].

1.1 Environmental impact

Coal has long dominated global power generation, but its environmental consequences are increasingly clear [13-15]. Emissions of SO₂ peaked in the late 20th century across the EU and U.S. before declining significantly with the enforcement of stringent air quality standards, installation of flue gas desulphurisation units, and retirement of older coal-fired plants [16]. By contrast, Asian economies, particularly China and India, have experienced rising SO₂ emissions in recent decades owing to rapid industrialisation and heavy dependence on coal.

Recently, policy interventions and clean energy programmes have begun to moderate this upward trend. Alongside SO₂, global CO₂ emissions from coal combustion have also increased. After decades of growth, CO₂ levels are beginning to decline as countries accelerate their decarbonisation and transition towards low-carbon energy sources. This trend is reflected in Figure 2, which shows the global coal-related CO₂ emissions over the past two decades [5].

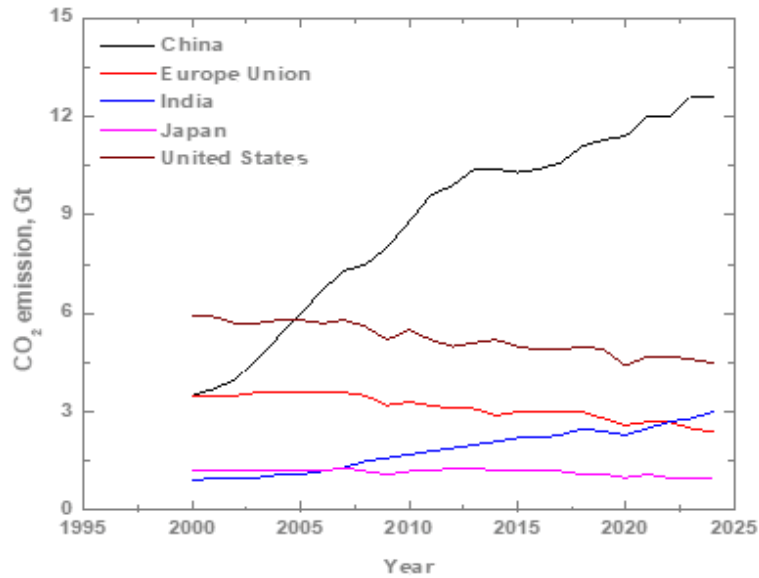


Figure 2. Global CO₂ emissions from coal combustion [3]

India mirrors these global dynamics, although with additional complexities. From a modest 1,362 MW installed capacity in 1947, India’s power generation capacity expanded to over 147,000 MW by 2008, with coal continuing to supply more than 70 % of the electricity demand [17]. Much of this coal is of inferior quality, characterised by high ash and low calorific value (CV), while better grades are diverted to steel and other industries. The use of poor-grade coal aggravates SO₂ pollution, particularly across the Indo-Gangetic plain and eastern states [18; 19]. Between 1980 and 2020, the expansion of thermal plants has caused a steep rise in SO₂ emissions. Similarly, Figure 3 illustrates India’s coal-based CO₂ emissions between 2008 and 2025, which follow a strong upward trajectory until the last few years, when renewable adoption and national climate policies began to slow and eventually reverse the trend [20].

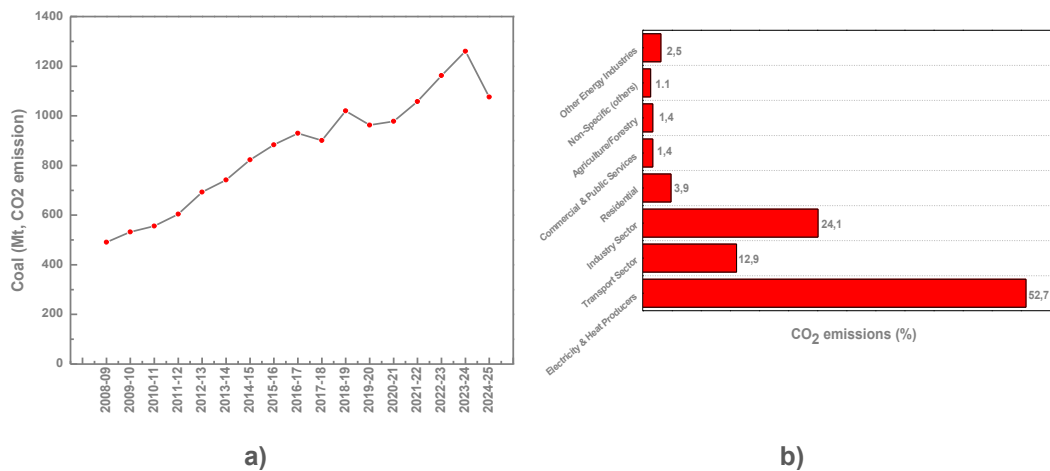


Figure 3. a) trend of coal-based CO₂ emissions in India (2008–2025); and b) major sectors contributing towards CO₂ emission [20]

The pressing challenge of rising emissions has underscored the urgency to scale-up renewable energy sources. Bioenergy has emerged as a key alternative energy source. Derived from agricultural residues, forestry byproducts, and other biomass resources, it can be transformed into useful energy via biochemical, thermochemical, or physicochemical routes [21]. This provides a low-carbon substitute for conventional fossil fuels and contributes to global decarbonisation. The expansion of renewable heat supplies, including bioenergy, is illustrated in Figure 4.

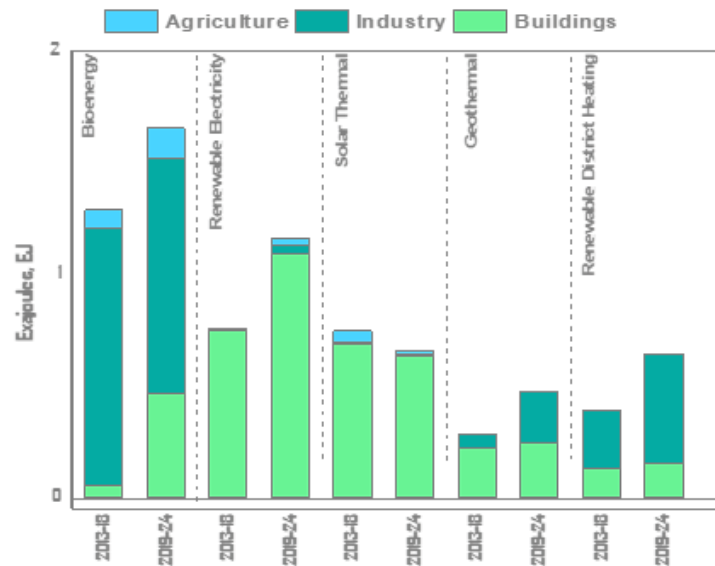


Figure 4. Growth in renewable energy consumption for heat, International Energy Agency, IEA (2013–2024)

1.2 Importance of co-firing

Co-firing refers to the concurrent use of coal and renewable or alternative fuels such as biomass within a single combustion unit for energy production. Co-firing is especially appealing in situations with limited financial and infrastructural capacity because it enables the continued use of existing coal-based facilities with only minor system adjustments. Several plants worldwide have been modified to conduct co-firing trials, generating operational evidence for their technical feasibility and reliability. This method is widely accepted as a decarbonisation tool because it requires relatively low capital investment while extending the usefulness of the existing coal infrastructure [22-25].

Biomass feedstock typically includes wood, wood waste, and residues from agriculture and forestry. In many regions, forest residues provide more than 70 % of the dry biomass potential [26]. Woody biomass composed of lignin and carbohydrates from branches, bark, roots, and leaves can be converted into energy via combustion, pyrolysis, gasification, and other thermochemical processes [27]. Depending on the technology, co-firing can be implemented as direct, indirect, or parallel firing with blending ratios of 5-10 % to ensure operational stability. The benefits are extensive: reduced CO₂, NO_x, and SO_x emissions, better utilisation of waste biomass, improved energy security, and lower fossil fuel costs [4].

International experience provides strong evidence of its viability. The Netherlands pioneered large-scale co-firing trials in the 1990s, achieving a biomass share of up to 30 % in ultra-supercritical units integrated with carbon capture. Finland operates the world's largest circulating fluidised bed boiler (550 MW), which is capable of flexible coal–biomass firing, whereas the UK has converted several coal stations to co-firing, with a total installed capacity exceeding 25 GW by 2018. Comparative life-cycle assessments across Europe and the U.S. have reported greenhouse gas reductions of up to 76 % compared with coal-only generation. Global reviews further confirm that biomass co-firing is a proven cost-effective bridge

technology in clean energy transition [28; 29]. Additionally, torrefaction has gained international traction as a pretreatment method, producing a coal-like solid fuel with higher energy density, lower moisture content, and superior grindability, enabling higher co-firing shares [30]. India’s pathways mirror these global practices. With a national mandate requiring biomass co-firing in coal plants beginning in 2022, blending levels of 5 % and, in some cases, 7 % have been demonstrated, such as at the National Thermal Power Corporation (NTPC) Dadri station [9]. This policy not only reduces stubble burning by utilizing agricultural residues but also aligns India with the experiences of the EU, UK, Japan, and North America, where co-firing has been proven both technically and economically viable [3;4; 9; 30]. By capitalising on its vast biomass potential, India has embedded co-firing as a cornerstone of its clean energy transition. These global experiences demonstrate that co-firing is not only technically feasible, but also strategically significant, setting the stage for a broader discussion of its role as a sustainable approach to clean energy. Table 1 summarises the main biomass conversion pathways, their feedstocks, and the associated energy outputs [31-33].

Table 1. Classification of biomass conversion technologies based on process, feedstock, and end products

Process	Technology	Feedstock	Usable end product
thermochemical conversion	combustion	agricultural residues woody residues animal wastes	heat electricity
	pyrolysis	agricultural residues woody residues	pyrolysis oil producer gas char
	gasification	agricultural residues woody residues	producer gas liquid fuels char
	liquefaction	agricultural residues algal biomass	fertilizer/biofuel syngas liquid fuels
biochemical conversion	anaerobic digestion	animal wastes sewage sludge	liquid fuels biogas electricity
	fermentation	agricultural residues sugars starch	liquid fuels (bioethanol)
physicochemical conversion	esterification/transesterification	vegetable oils animal fats waste oils	liquid fuels glycerol

1.3 Biomass co-firing – a sustainable approach

Biomass co-firing is a well-established and widely adopted approach for reducing emissions from coal-based power plants amid growing environmental concerns. Recognised by the United Nations Framework Convention on Climate Change as a carbon-neutral energy source, biomass enables co-firing to function as a practical, cost-effective, and sustainable strategy for emission mitigation using existing coal infrastructure [34]. By leveraging the established energy conversion pathways, co-firing reduces reliance on coal without major system modifications. Globally, co-firing implementation varies, but follows the common goal of increasing renewable penetration. In the EU, the Renewable Energy Directive (RED III) mandates higher renewable shares with certified biomass as a key component. The UK has demonstrated large-scale deployment through plants such as Drax, which has transitioned predominantly to biomass under stringent sustainability criteria. In Japan, biomass co-firing is incentivised through the Feed-in Tariff, which promotes fuels, such as wood pellets and palm kernel shells, alongside pilot initiatives on ammonia co-firing. In North America, the co-firing trials of pulverised coal

and fluidised bed plants are supported by Renewable Portfolio Standards and regional carbon regulations [3; 4].

Recent studies have confirmed the long-term viability of co-firing. Indonesian trials showed that blending rice husk (RH) and sawdust (SD) with coal improved combustion efficiency while reducing air requirements and emissions [35]. Japanese studies emphasised the optimisation of woody biomass supply chains to balance energy efficiency, economic performance, and environmental impacts [36]. In the U.S., assessments indicate that integrating biomass with waste coal and carbon capture can reduce CO₂ emissions by more than 80 %, with some co-firing ratios achieving a negative global warming potential [37], positioning co-firing as a critical pathway towards carbon neutrality.

In India, co-firing adoption has accelerated beyond minimum mandates. The NTPC demonstrated 7 % biomass blending at the Dadri thermal power plant, confirming its technical feasibility. Biomass pellets are compatible with existing pulverisation systems, such as bowl mills, vertical roller mills, and beater mills. Supporting this transition, the Government of India launched the Sustainable Agrarian Mission on the Use of Agro Residue in Thermal Power Plants (SAMARTH) Mission to reduce stubble burning, mitigate air pollution, and strengthen biomass integration into the power grid [34; 38].

Policy revisions have accelerated their deployment. The Ministry of Power updated its biomass co-firing mandate on June 16, 2023 requiring 5 % blending from 2024-2025 and 7 % by 2025-2026 [9]. State-wise adoption varied, with Uttar Pradesh leading at 70,977 Mt, followed by Maharashtra (27,349 Mt), Haryana (20,969 Mt), and Madhya Pradesh (17,600 Mt). Biomass co-firing has been implemented across 47 thermal power plants nationwide, with a cumulative utilisation of 164,976 Mt. These initiatives demonstrate India's alignment with global best practices while delivering socio-economic benefits through agricultural residue utilisation. To further enhance the biomass quality and enable higher substitution ratios, pretreatment technologies such as torrefaction are increasingly adopted worldwide for efficient co-firing applications.

1.4 Benefits of the torrefaction

Torrefaction is a mild thermochemical pretreatment process in which biomass is gradually heated in an oxygen-limited or inert environment to improve its fuel properties. This process is typically carried out at temperatures below 300 °C, resulting in a more energy-dense, hydrophobic, and coal-like material suitable for energy applications. This process decreases the inherent moisture content, enhances energy density, and yields a uniform and stable solid fuel with improved grindability, handling, and storage characteristics [39; 40]. Based on the reaction environment, torrefaction is broadly classified into non-oxidative torrefaction, which is performed in the absence of oxygen, and oxidative torrefaction, where controlled oxygen availability enables partial oxidation and thermal degradation. Previous studies have shown that woody biomass generally exhibits greater structural resilience under oxidative torrefaction than fibrous feedstocks [41]. Experimental studies further demonstrated that key operating variables, including temperature, residence time, and oxygen concentration, govern the extent of biomass transformation. For example, torrefaction of sewage sludge at 300 °C for 1 h resulted in moisture levels below 3 % and an increase in fixed carbon to approximately 65 % [42]. Similarly, steam-assisted torrefaction of SD enhanced the pellet density and CV [43], whereas comparative studies on *Gliricidia* and rubberwood revealed complementary improvements in the carbon content and heating value [44]. Additional research on corn stover, coffee grounds, coconut shells, and sugarcane bagasse (SCB) highlights the effectiveness of torrefaction in upgrading low-value biomass residues into energy-rich fuels [45-47].

The application of torrefied biomass in coal-fired power plants has demonstrated consistent operational and environmental benefits. At the Seward Station in the U.S., torrefied SD co-firing led to improved power output [48], whereas wheat straw blends reduced emissions, albeit with minor operational modifications [49]. Stable electricity generation using locally sourced torrefied residues was also demonstrated at King Station [50]. Enhanced biomass reactivity following torrefaction has been linked to improved boiler performance and lower NO_x emissions

[16]. Similar trends have been reported globally: Indonesian studies showed that torrefied RH and SD improved combustion efficiency [35]; Japanese system analyses confirmed reductions in cost and CO₂ emissions through optimised supply chains for torrefied woody biomass [36]; and U.S. assessments reported CO₂ reductions exceeding 80 % when torrefied pine was co-fired with waste coal in conjunction with carbon capture and storage systems [37].

Beyond power generation, torrefaction supports broader biomass valorisation pathways. Municipal solid waste has been converted into biochar through torrefaction [51], whereas agro residues such as coffee husks and cocoa shells have demonstrated suitability as co-firing fuels [52]. This process also complements pyrolysis by producing high-calorific char from cotton stalks [53] and enhancing thermal stability through hemicellulose decomposition [54]. Modelling studies suggest that torrefaction temperatures in the range of 230-270 °C are optimal for maximising energy yield from Calliandra wood pellets [55]. From a policy perspective, carbon pricing instruments such as CO₂ taxation have been shown to be more effective than generalised energy taxes in accelerating biomass utilisation [56], whereas the expansion of biofuel markets, including ethanol, biodiesel, and biomethane, further strengthens the relevance of torrefaction [57]. Recent investigations involving Kraft pulp sludge [58] and spruce SD [59] also confirmed the ability of the process to improve fuel stability and quality.

Globally, torrefaction is gaining prominence as a key component of decarbonisation strategies in regions such as the EU, the U.S., Japan, and India, owing to its ability to enhance biomass fuel quality, enable higher substitution levels in coal-based systems, and reduce challenges related to handling, storage, and transport. In India, the widespread availability of biomass residues, including SD, SCB, and RH positions torrefaction as a promising pathway for aligning indigenous resources with international clean energy goals. Against this backdrop, this study examined the fuel-upgrading potential of these three biomass feedstocks through torrefaction, selected for their renewability, regional abundance, and strategic relevance to India's biomass-driven energy transition. The distinct contribution of this study lies in its systematic evaluation of oxidative torrefaction under ambient air conditions, which offers a cost-effective and operationally realistic alternative to conventional inert atmosphere treatments. Through a comparative analysis of thermal behaviour, chemical modification, and fuel property enhancement, this study provides feedstock-specific insights that directly support biomass co-firing applications and bridge laboratory-scale thermochemical processing with large-scale low-emission energy deployment in coal-fired power systems.

2 Methodology

2.1 Biomass collection

Three commonly available biomass types, SCB, SD, and RH, were selected for this study because of their regional abundance and relevance in bioenergy applications. Fresh SCB was obtained from a sugarcane refreshment hub in Chinnampalayam, Coimbatore. SD and RH were collected from a local sawmill and rice mill, respectively, in the same locality.

2.2 Figures

Torrefaction experiments were conducted using a laboratory muffle furnace to investigate the thermal behaviour and fuel enhancement potential of the selected biomass types. Prior to torrefaction, the biomass samples were washed with deionised water, oven-dried at 105 °C for 24 h, and ground to a particle size range of 250-500 µm. For each trial, 10 g of biomass was placed in ceramic crucibles and torrefied at 200, 250, and 300 °C for 30 min under ambient air conditions to simulate oxidative torrefaction [53; 60] as shown in Figure 5. After treatment, the crucibles were cooled in a furnace to minimise oxidative degradation due to sudden air exposure.

The post-torrefaction samples were analysed for mass yield, proximate composition (moisture, volatile matter, ash, and fixed carbon), and CV using standard ASTM protocols [61-63] and bomb calorimetry [64]. Comparative torrefaction was also conducted under a nitrogen

atmosphere to examine the effects of oxidative and inert conditions on the biomass characteristics.

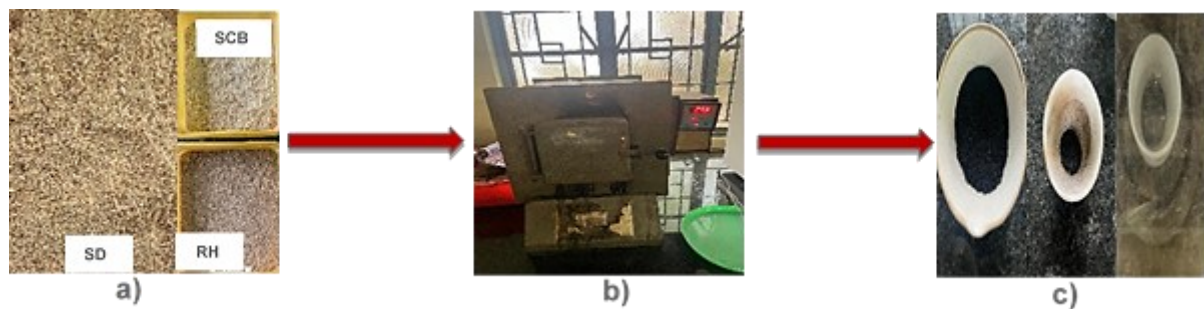


Figure 5. Schematic representation of the torrefaction process: a) raw material; b) torrefaction process; and c) torrefied sample

2.3 Visual characterization

The biomass samples torrefied at different temperatures were visually compared. Progressive darkening, shrinkage, and structural breakdown were observed with increasing torrefaction temperatures, indicating enhanced carbonisation and degradation of hemicellulose and cellulose [65-67].

2.4 Proximate analysis of biomass

All proximate analyses were performed in triplicate and the reported results represent the average values. Moisture content was determined in accordance with ASTM D4442-16 by oven-drying biomass samples at 105 °C until constant mass was achieved. Ash content was measured following ASTM E1755-01 by combusting the samples at 760 °C to obtain residual inorganic matter. The volatile matter was evaluated according to ASTM E872-82 by subjecting the samples to high-temperature heating for a specified duration. The fixed carbon content was subsequently estimated indirectly from the measured moisture, ash, and volatile matter contents following standard proximate analysis procedures [68].

2.5 CV determination

The higher heating value of the biomass was measured using a bomb calorimeter. The samples were combusted in a pressurised oxygen environment within a sealed metal chamber submerged in a water bath. The resulting increase in temperature was recorded to calculate the CV.

2.6 Elemental analyses

Elemental analysis was performed using energy dispersive X-ray spectroscopy (EDS) to assess the elemental composition of the biomass, including C, O, N, and S. Although EDS is semi-quantitative and less accurate for light elements (C, O, and N), it provides valuable surface-level insights. EDS detects the characteristic X-rays emitted from a sample upon excitation by an electron beam [69].

2.7 Fourier Transform Infrared (FTIR) analysis

FTIR spectroscopy was used to identify the chemical functional groups on the biomass surface. The dried samples were scanned across a range of 400-4000 cm^{-1} with a step size of 4 cm^{-1} and a scan rate of 40 scans per sample [60; 70]. The resulting spectra were analysed to detect the structural and chemical changes induced by torrefaction.

2.8 Thermogravimetric Analysis (TGA)

TGA was employed to assess the thermal stability and decomposition behaviour of the raw and torrefied biomass. The samples were subjected to a controlled heating program under

both air and nitrogen atmospheres, and the weight loss was recorded as a function of temperature to characterise moisture evaporation, volatile release, and thermal degradation [71].

3 Results and discussion

3.1 Visual changes and thermal torrefaction

The torrefaction of SCB, SD, and RH was successfully carried out at three temperature levels (200, 250, and 300 °C) for 30 min under oxidative conditions, as illustrated in Figure 6. All biomass types exhibited clear visual and physical transformations post-treatment, including progressive darkening of colour, shrinkage, and brittleness, indicating increased degrees of thermal decomposition and carbonisation. At 200 °C, only mild changes were observed: the samples retained much of their original colour and structure, suggesting partial devolatilisation and minimal hemicellulose degradation. As the temperature increased to 250 °C, biomass darkening intensified, with noticeable mass loss and shrinkage. This stage represents the onset of significant hemicellulose breakdown and the increased formation of intermediate volatile compounds. At 300 °C, the torrefied samples turned distinctly dark brown to black, with visibly charred surfaces and enhanced brittleness. Surface changes and brittleness are correlated with the extensive thermal degradation of hemicellulose and cellulose, increased fixed carbon formation, and moisture/volatile matter loss, resulting in an upgraded fuel-like character. Such structural changes are consistent with prior studies on oxidative torrefaction [53; 72], where elevated temperatures led to an increased carbon concentration and reduced hydrophilic behaviour of the biomass.



Figure 6. Visual changes in biomass during oxidative torrefaction at 200, 250, and 300 °C

3.1.1 Cooling strategy and oxidative control

To prevent post-torrefaction oxidation, the ceramic crucibles were cooled in the furnace and gradually returned to room temperature under reduced airflow. This step is critical for avoiding the unwanted combustion or re-oxidation that may occur when hot, carbon-rich samples are exposed directly to ambient air. The visual uniformity and surface integrity of the torrefied samples confirmed the effectiveness of the controlled cooling strategy.

3.1.2 Implications for fuel enhancement

The temperature-dependent behaviour of the biomass samples indicates that torrefaction at 300 °C for 30 min offers the most significant improvement in fuel quality, with higher fixed carbon, lower moisture, and enhanced combustion potential as shown in Figure 7. These findings align with the trends observed in the calorimetric and proximate analyses, as discussed in subsequent sections.

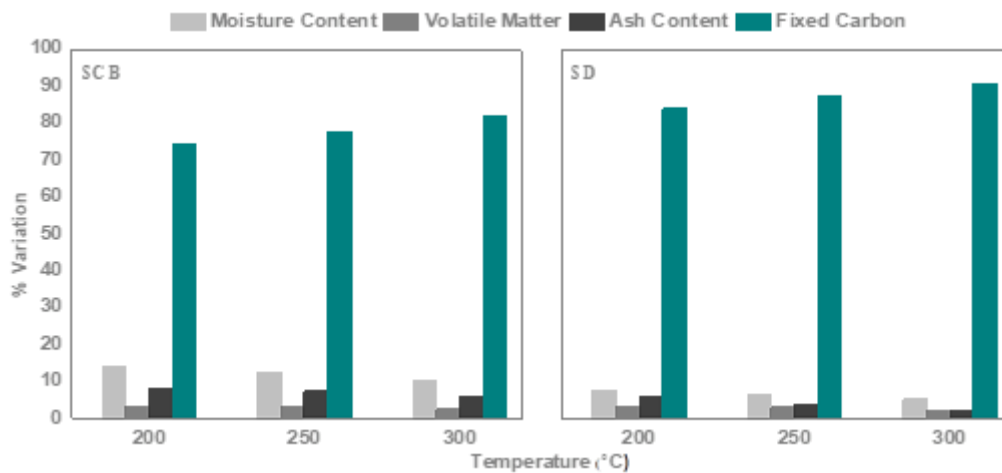


Figure 7. Effect of torrefaction temperature on proximate composition of SCB and SD

3.2 Proximate analysis and CV

Table 2 presents a comparative analysis of non-torrefied and torrefied SCB, SD, and RH concerning proximate composition, combustion efficiency, and CV at 300 °C. In the raw state, the three biomass feedstocks exhibited distinct combustion characteristics. SCB contained 10,04 % moisture, 10,82 % ash, and 4,86 % volatile matter, resulting in a fixed carbon content of 74,28 % and CV of 4138,72 kcal/kg. SD showed superior combustion properties, with lower moisture (5,87 %) and ash content (6,03 %) and a higher fixed carbon percentage (83,09 %) than SCB. Its CV was correspondingly higher at 4261,01 kcal/kg. In contrast, RH presents the highest ash content (15,54 %) and lowest CV (3593,43 kcal/kg), indicating reduced fuel quality owing to its significant silica content [30; 73].

Table 2. Effect of torrefaction at 300 °C on fuel properties of SCB, SD, and RH

S No.	Category	Raw material	Moisture content (%)	Volatile matter (%)	Ash content (%)	Fixed carbon (%)	Combustion efficiency	Calorific value (kcal/kg)
1	Non-torrefied	SCB	10,04	4,86	10,82	74,28	93,898	4138,72
2		SD	5,87	5,01	6,03	83,09	96,462	4261,01
3		RH	8,94	2,40	15,54	73,12	93,976	3593,43
4	Torrefied at 300 °C	SCB	8,65	2,56	5,18	83,61	95,157	5369,01
5		SD	5,72	1,08	2,36	90,84	96,904	5941,53
6		RH	7,87	1,70	8,05	82,38	95,260	3538,50

Torrefaction at 300 °C substantially enhanced the fuel properties of SCB and SD. For SCB, the moisture content was reduced to 8,65 %, ash content decreased to 5,18 %, and fixed carbon increased to 83,61 %. The reduction in moisture, ash content, and fixed carbon content resulted in a 29,70 % increase in the CV, rising to 5369,01 kcal/kg. SD showed the most significant improvement, with moisture reduced to 5,72 %, ash content reduced to 2,36 %, and fixed carbon content reaching 90,84%. Its CV increases to 5941,53 kcal/kg, making it the most efficient of the tested samples [72; 74]. RH demonstrated moderate improvements post-torrefaction. The moisture content decreased to 7,87 % and the fixed carbon content increased to 82,38 %. However, its CV slightly declines to 3538,50 kcal/kg. This outcome is likely due to the persistence of high ash and silica contents, which limit the energy yield despite carbon enrichment. These findings suggest that although torrefaction improves the combustion properties of all biomass types, the degree of enhancement varies based on the inherent

characteristics of each material. SD has emerged as the most suitable candidate for co-firing applications because of its superior energy density and low ash content after torrefaction.

3.3 Elemental analysis

The EDS analysis was performed to examine the elemental composition of SCB, SD, and RH before and after torrefaction. The results summarised in Table 3 highlight the changes in the carbon, oxygen, nitrogen, sulfur, and silicon contents resulting from the thermal treatment. For SCB, the carbon content increased from 69,08-72,76 % after torrefaction, reflecting the removal of volatile components, leading to carbon enrichment in the solid phase. Concurrently, the oxygen content decreased from 29,08-24,66, which is consistent with the release of oxygen-rich volatiles such as water vapour, carbon monoxide, and carbon dioxide during torrefaction. The nitrogen content slightly increased from 1,85-2,57 %, which may be attributed to nitrogen fixation or the concentration of stable nitrogenous compounds. Sulfur levels remained constant at 0,01 %, suggesting minimal transformation of sulfur-containing elements in the SCB. No detectable silicon was observed in either the raw or torrefied SCB samples. For SD, the results deviated from typical torrefaction trends. Carbon content decreased unexpectedly from 72,18-58,42 %, whereas oxygen content increased from 26,07-39,06 %. This anomaly could be due to several factors, including uneven thermal exposure, sample heterogeneity, and possible oxidation of the partially torrefied material. The nitrogen content increased from 1,74-2,50 %, whereas sulfur remained constant at 0,01 %, similar to that of SCB. Silicon was undetectable in both the raw and torrefied SD samples. For RH, torrefaction led to a moderate increase in the carbon content from 26,55-33,22 %, whereas the oxygen content significantly decreased from 71,79-51,30 %, indicating typical devolatilisation behaviour. The nitrogen content exhibited a slight reduction from 1,59-1,39 %, and sulfur levels dropped from 0,07-0,01 %, indicating minimal sulfur retention. Notably, silicon, which was undetectable in the raw RH, emerged prominently after torrefaction at 14,08 %. This increase likely results from the relative concentration of inorganic components as the organic matrix decomposes, a phenomenon commonly observed in silica-rich biomass such as RH. These findings confirm that torrefaction significantly alters the elemental composition of biomass, primarily by increasing the carbon concentration and reducing the oxygen content. However, the extent of change is dependent on the biomass type and structure. The unusual behaviour observed in SD suggests the need for further investigation into torrefaction conditions, particularly temperature uniformity and exposure time, to optimise fuel quality.

Table 3. Elemental composition of biomass samples before and after torrefaction (EDS analysis)

Biomass	Reference	C (%)	O (%)	N (%)	S (%)	Si (%)
SCB	Non-torrefied	69,08	29,08	1,85	0,01	NA
	Torrefied	72,76	24,66	2,57	0,01	NA
SD	Non-torrefied	72,18	26,07	1,74	0,01	NA
	Torrefied	58,42	39,06	2,50	0,01	NA
RH	Non-torrefied	26,55	71,79	1,59	0,07	NA
	Torrefied	33,22	51,30	1,39	0,01	14,08

3.4 FTIR analysis

FTIR was used to analyse the chemical and structural transformations in SCB, SD, and RH resulting from torrefaction. The FTIR spectra shown in Figure 8 reveal changes in the functional groups, reflecting molecular breakdown, bond rearrangement, and compositional shifts induced by heat treatment [75; 76]. In the non-torrefied samples, all biomass types exhibited characteristic peaks corresponding to lignocellulosic structures.

SCB showed strong absorptions at $3341,07\text{ cm}^{-1}$ (O–H and C–H stretching), $2893,66\text{ cm}^{-1}$ (CH_2 groups), and $1724,05\text{ cm}^{-1}$ (C=O stretching in hemicellulose and lignin). Peaks at $1244,83\text{ cm}^{-1}$ and $1034,62\text{ cm}^{-1}$ confirmed the presence of carbohydrates like cellulose. A distinct low-frequency band at $417,51\text{ cm}^{-1}$ suggested presence of zinc oxide, possibly due to contamination.

For SD, similar lignocellulosic features were observed with O–H stretching at $3716,16\text{ cm}^{-1}$ and $3340,1\text{ cm}^{-1}$, and unsaturated C=C stretches at $3019,98\text{ cm}^{-1}$ and $1442,49\text{ cm}^{-1}$. Carbonyl vibrations at $1739,48\text{ cm}^{-1}$ and C–O bonds at $1020,16\text{ cm}^{-1}$ indicated cellulose and hemicellulose content, and a $525,51\text{ cm}^{-1}$ Cu–O stretch suggested metallic traces. RH exhibited dominant O–H stretching at $3577,31\text{ cm}^{-1}$, aliphatic C–H at $2954,41\text{ cm}^{-1}$, and nitrile $\text{C}\equiv\text{N}$ at $2122,28\text{ cm}^{-1}$. Peaks at $1738,51\text{ cm}^{-1}$ (C=O) and $1216,86\text{ cm}^{-1}$ (P=O) confirmed the presence of hemicellulose and phosphorus compounds, while $1008,59\text{ cm}^{-1}$ reflected carbohydrate C–O stretching. After torrefaction, all samples showed substantial spectral changes, indicative of chemical restructuring.

In SCB, new peaks appeared at $3801,97\text{ cm}^{-1}$ and $3461,6\text{ cm}^{-1}$, reflecting modifications in hydroxyl groups. The emergence of peaks at $3020,94\text{ cm}^{-1}$ (lipid-associated C–H stretching), $1737,55\text{ cm}^{-1}$ (C=O), and $1592,91\text{ cm}^{-1}$ (aldehydes) points to lignocellulose degradation. The disappearance of the ZnO signal implies changes in the inorganic phase. SD exhibited peak shifts in O–H stretching to $3461,6\text{ cm}^{-1}$ and $3014,19\text{ cm}^{-1}$, alongside the appearance of $1590,02\text{ cm}^{-1}$ (C–C bonding), $1436,71\text{ cm}^{-1}$ (CO groups), and $1367,28\text{ cm}^{-1}$ (alkanes). The presence of peaks at $1218,79\text{ cm}^{-1}$ and $1011,48\text{ cm}^{-1}$ indicates residual macromolecular structures. The loss of the Cu–O signal confirmed the alterations in the trace metal content.

For RH, new peaks at $3776,9\text{ cm}^{-1}$ and $3596,59\text{ cm}^{-1}$ were linked to altered O–H stretching, and peaks at $3013,23\text{ cm}^{-1}$ (C=C) and $2131,92\text{ cm}^{-1}$ ($\text{C}\equiv\text{C}$ alkyne) reflected the formation of unsaturated bonds. The retention of the $1738,51\text{ cm}^{-1}$ carbonyl band and new CN stretching at $908,31\text{ cm}^{-1}$ signify both degradation and structural rearrangement. The persistence of phosphorus signals highlighted the selective retention of the inorganic components.

Overall, the FTIR analysis confirmed that torrefaction induced significant molecular changes across all biomass types. The reduction of hydroxyl groups, the formation of aldehydes, ketones, and alkanes, and the emergence of unsaturated bonds suggested the breakdown of polysaccharides and lignin into more stable, energy-dense compounds. The alteration of inorganic spectral features, including the disappearance of the ZnO and CuO peaks and the persistence of phosphorus in the RH, indicated changes in the mineral composition after torrefaction. These transformations enhance the CV and improve the fuel characteristics of biomass, thereby supporting its use in thermal energy applications.

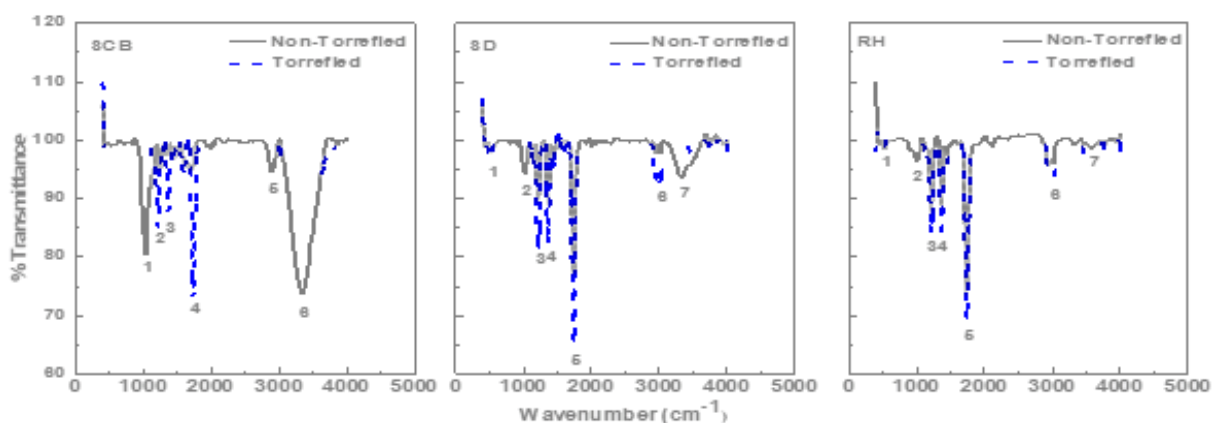


Figure 8. FTIR spectra of raw and torrefied SCB, SD, and RH showing functional group changes

3.5 TGA analysis

TGA was conducted to assess the thermal decomposition behaviours of SCB, SD, and RH before and after torrefaction. All samples were analysed under identical conditions using a Pyris 6 TGA instrument with a nitrogen flow of 20,0 mL/min, a heating rate of 10 °C/min, and a final temperature of 850 °C. The thermograms shown in Figures 9-11 illustrate the distinct differences in thermal stability between the non-torrefied and torrefied samples. For SCB, the non-torrefied sample exhibited a 44,93 % weight loss at 351,71 °C due to the decomposition of hemicellulose and cellulose. In comparison, the torrefied sample showed only an 11,25 % weight loss at 333,08 °C, retaining 88,75 % of its mass, indicating significant volatile matter removal and carbon enrichment. Similarly, SD demonstrated improved stability after torrefaction, with the non-torrefied sample retaining 88,078 % of its mass at 329,75 °C and the torrefied sample retaining 92,779 % at 346,88 °C, reflecting reduced volatile matter content and increased fixed carbon content. In the case of RH, the non-torrefied sample lost 32,036 % of its mass at 355,02 °C. However, the torrefied RH exhibited no distinct decomposition peaks, indicating gradual weight loss and enhanced thermal stability due to prior devolatilisation. Across all biomass types, torrefaction significantly reduced the moisture and volatile matter contents, leading to greater thermal resistance and higher energy density. These results confirm that torrefied biomass is more suitable for combustion and co-firing applications, offering improved fuel characteristics and an increased fixed carbon content.

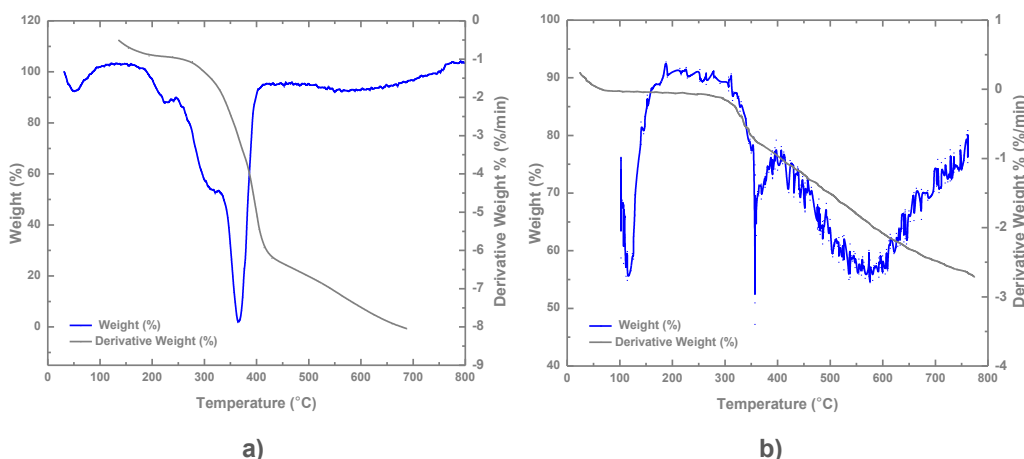


Figure 9. TGA thermograms of: a) non-torrefied; and b) torrefied sugarcane bagasse (SCB) under nitrogen atmosphere

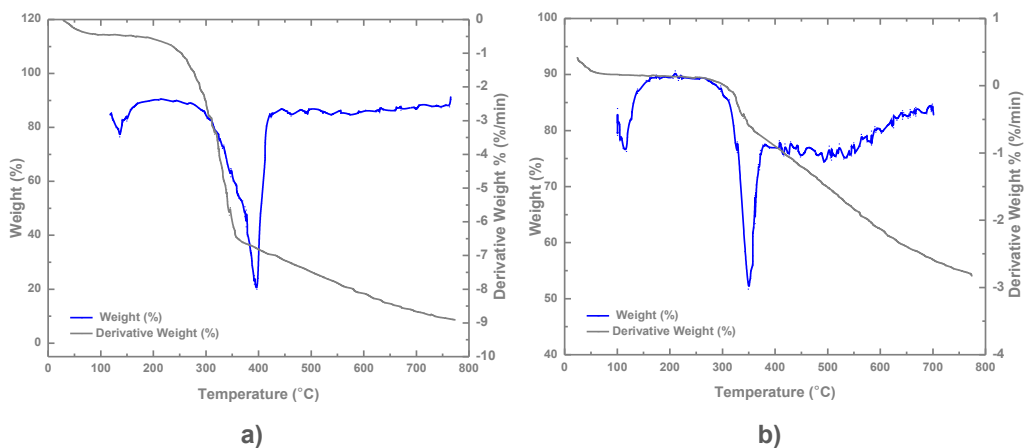


Figure 10. TGA thermograms of: a) non-torrefied; and b) torrefied rice husk (RH) under nitrogen atmosphere

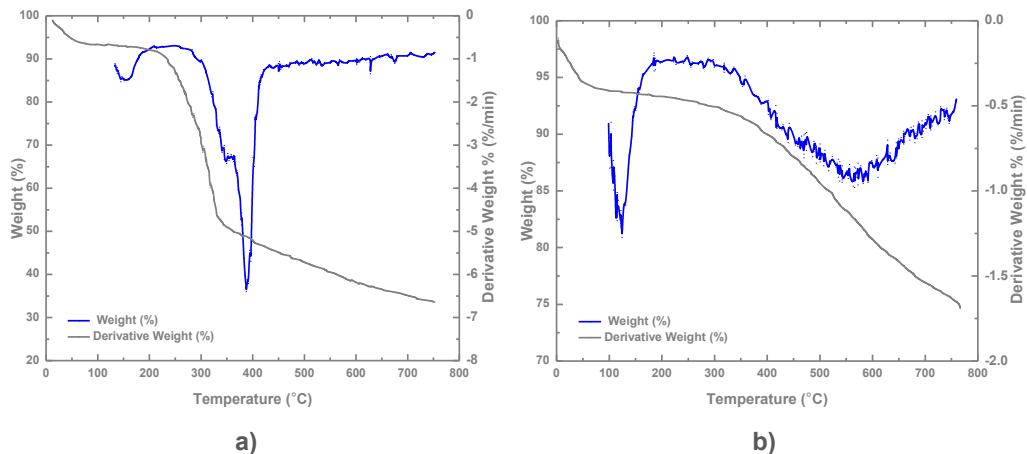


Figure 11. TGA thermograms of: a) non-torrefied; and b) torrefied rice husk (RH) under nitrogen atmosphere

4 Conclusion

This study comprehensively evaluated the thermal, chemical, and structural transformations of SCB, SD, and RH subjected to oxidative torrefaction at temperatures of 200, 250, and 300 °C. Visual inspection confirmed progressive darkening, shrinkage, and brittleness of the biomass, especially at 300 °C, indicating substantial devolatilisation and carbonisation. Proximate analysis and CV assessments revealed significant improvements in fuel quality, with reductions in moisture and ash content and increases in fixed carbon and CV. SD exhibited the most favourable response to torrefaction, achieving the highest CV of 5941,53 kcal/kg and minimal ash content, making it the most efficient biomass for co-firing applications. Elemental analysis using EDS demonstrated increased carbon concentrations and reduced oxygen content in the SCB and RH after torrefaction. However, the SD showed anomalous trends owing to potential heterogeneity or uneven heat exposure. FTIR analysis confirmed the breakdown of hemicellulose and lignin, formation of energy-rich alkanes and aldehydes, and structural changes in the polysaccharides. Also, selective retention or transformation of inorganic elements, such as silicon and phosphorus, was observed. TGA further validated these findings, showing reduced weight loss in the torrefied samples and enhanced thermal stability due to prior volatile removal. Collectively, these results indicate that oxidative torrefaction at 300 °C significantly improved the combustion characteristics, energy density, and stability of lignocellulosic biomass, particularly SD and SCB. This suggests a viable pathway for integrating torrefied biomass into co-firing systems, contributing to cleaner energy production and reduced reliance on fossil fuels in India's thermal power sector.

Future research should focus on optimising torrefaction parameters, including temperature, residence time, and atmospheric conditions tailored to specific biomass types to maximise energy yield and minimise environmental impacts. Pilot- and industrial-scale co-firing trials are essential for evaluating the real-world performance of torrefied biomass blended with various grades of coal, particularly in terms of combustion efficiency, emission profiles, slagging, and fouling tendencies. Additionally, comprehensive life cycle assessments and techno-economic analyses are critical for determining the environmental sustainability and commercial viability of large-scale torrefaction and co-firing systems. The incorporation of catalysts or additives during torrefaction offers a promising approach for enhancing fuel properties, lowering processing temperatures, and improving process efficiency. Further investigations into material compatibility, storage stability, and supply chain logistics are recommended to facilitate the large-scale deployment of torrefied biomass in energy applications.

References

- [1] Akerboom, S. et al. Meeting goals of sustainability policy: CO₂ emission reduction, cost-effectiveness and societal acceptance. An analysis of the proposal to phase-out coal in the Netherlands. *Energy Policy*, 2020, 138, 111210. <https://doi.org/10.1016/j.enpol.2019.111210>
- [2] Srivastav, S.; Zaehringer, M. The economics of coal phaseouts: auctions as a novel policy instrument for the energy transition. *Climate Policy*, 2024, 24 (6), pp. 754-765. <https://doi.org/10.1080/14693062.2024.2358114>
- [3] European Commission. Renewable Energy Directive (RED III). Official Journal of the European Union, 2023. Accessed: May 28, 2026. Available at: <https://eur-lex.europa.eu/eli/dir/2023/2413/oj/eng>
- [4] IEA Bioenergy Task 32. Status of large-scale biomass co-firing. IEA Bioenergy Report, 2021. Accessed: May 28, 2026. Available at: <https://www.ieabioenergy.com/blog/publications/the-status-of-large-scale-biomass-firing/>
- [5] International Energy Agency. Global Energy Review 2025. Accessed: July 10, 2025. Available at: <https://www.iea.org/reports/global-energy-review-2025>
- [6] BP. BP Statistical Review of World Energy 2019. Accessed: July 10, 2025. Available at: <https://www.bp.com/content/dam/bp/businesssites/en/global/corporate/pdfs/energy-economics/statistical-review/bp-stats-review-2019-full-report.pdf>
- [7] International Energy Agency. India Energy Outlook 2021 – Analysis. Accessed: July 10, 2025. Available at: <https://www.iea.org/reports/india-energy-outlook-2021>
- [8] Ministry of Power, Government of India. Revised Biomass Policy mandates 5% biomass co-firing in Thermal Power Plants from FY 2024-25: Union Minister for Power and New & Renewable Energy. Accessed: July 10, 2025. Available at: <https://pib.gov.in/PressReleaseIframePage.aspx?PRID=1945245>
- [9] Ministry of Statistics and Programme Implementation. Energy Statistics India 2024. Accessed: July 10, 2025. Available at: https://www.mospi.gov.in/sites/default/files/publication_reports/EnergyStatistics_India_publication_2024N.pdf
- [10] Bhuiyan, A. A.; Naser, J. Thermal characterization of coal/straw combustion under air/oxy-fuel conditions in a swirl-stabilized furnace: A CFD modelling. *Applied Thermal Engineering*, 2016, 93, pp. 639-651. <https://doi.org/10.1016/j.applthermaleng.2015.10.024>
- [11] Ian Barnes, D. Understanding pulverised coal, biomass and waste combustion – A brief overview. *Applied Thermal Engineering*, 2015, 74, pp. 89-95. <https://doi.org/10.1016/j.applthermaleng.2014.01.057>
- [12] Tillman, D. A.; Duong, D. N. N.; Harding, N. S. *Solid Fuel Blending: Principles, Practices, and Problems*. England: Elsevier, 2012.
- [13] Prakash, R.; Thenmozhi, R.; Raman, S. N. Mechanical characterisation and flexural performance of eco-friendly concrete produced with fly ash as cement replacement and coconut shell coarse aggregate. *International Journal of Environment and Sustainable Development*, 2019, 18 (2), pp. 131-148. <https://doi.org/10.1504/IJESD.2019.099491>
- [14] Prakash, R.; Srividhya, S.; Gowrishankar, V.; Kumar, S. S. Development of a novel sustainable concrete from waste coconut shell with alccofine supplements. *Advances in Civil and Architectural Engineering*, 2024, 15 (28), pp. 151-165. <https://doi.org/10.13167/2024.28.11>
- [15] Chandra Sekar, K.; Murugesan, R.; Sivaraja, M.; Prakash, R. Development of sustainable concrete from hypo sludge combined with basalt fibre and latex. *Sustainability*, 2023, 15 (14), 10986. <https://doi.org/10.3390/su151410986>

- [16] Gütschow, J. et al. The PRIMAP-hist national historical emissions time series. *Earth System Science Data*, 2016, 8 (2), pp. 571-603. <https://doi.org/10.5194/essd-8-571-2016>
- [17] Mishra, U. C. Environmental impact of coal industry and thermal power plants in India. *Journal of Environmental Radioactivity*, 2004, 72 (1-2), pp. 35-40. [https://doi.org/10.1016/S0265-931X\(03\)00183-8](https://doi.org/10.1016/S0265-931X(03)00183-8)
- [18] Avirneni, S.; Bandlamudi, D. Environmental impact of thermal power plant in India and its mitigation measure. *International Journal of Modern Engineering Research*, 2013, 3 (2), pp. 1026-1031.
- [19] Kuttippurath, J.; Patel, V. K.; Pathak, M.; Singh, A. Improvements in SO₂ pollution in India: Role of technology and environmental regulations. *Environmental Science and Pollution Research*, 2022, 29 (52), pp. 78637-78649. <https://doi.org/10.1007/s11356-022-21319-2>
- [20] NITI Aayog. India Energy – Electricity Generation. Accessed: July 10, 2025. Available at: <https://iced.niti.gov.in/energy/electricity/generation>
- [21] Adams, P. et al. Biomass conversion technologies. *Greenhouse Gas Balances of Bioenergy Systems*, 2018, pp. 107-139. <https://doi.org/10.1016/B978-0-08-101036-5.00008-2>
- [22] Tillman, D. A. Biomass co-firing: The technology, the experience, the combustion consequences. *Biomass and Bioenergy*, 2000, 19 (6), pp. 365-384. [https://doi.org/10.1016/S0961-9534\(00\)00049-0](https://doi.org/10.1016/S0961-9534(00)00049-0)
- [23] Hartmann, D.; Kaltschmitt, M. Electricity generation from solid biomass via co-combustion with coal: Energy and emission balances from a German case study. *Biomass and Bioenergy*, 1999, 16 (6), pp. 397-406. [https://doi.org/10.1016/S0961-9534\(99\)00017-3](https://doi.org/10.1016/S0961-9534(99)00017-3)
- [24] De, S.; Assadi, M. Impact of co-firing biomass with coal in power plants – A techno-economic assessment. *Biomass and Bioenergy*, 2009, 33 (2), pp. 283-293. <https://doi.org/10.1016/j.biombioe.2008.07.005>
- [25] Roni, M. S. et al. Biomass co-firing technology with policies, challenges, and opportunities: A global review. *Renewable and Sustainable Energy Reviews*, 2017, 78, pp. 1089-1101. <https://doi.org/10.1016/j.rser.2017.05.023>
- [26] Van Belle, J.-F.; Temmerman, M.; Schenkel, Y. Three level procurement of forest residues for power plant. *Biomass and Bioenergy*, 2003, 24 (4-5), pp. 401-409. [https://doi.org/10.1016/S0961-9534\(02\)00161-7](https://doi.org/10.1016/S0961-9534(02)00161-7)
- [27] Vassilev, S. V. et al. An overview of the organic and inorganic phase composition of biomass. *Fuel*, 2012, 94, pp. 1-33. <https://doi.org/10.1016/j.fuel.2011.09.030>
- [28] Xu, Y.; Yang, K.; Zhou, J.; Zhao, G. Coal-biomass co-firing power generation technology: Current status, challenges and policy implications. *Sustainability*, 2020, 12 (9), 3692. <https://doi.org/10.3390/su12093692>
- [29] Beagle, E.; Belmont, E. Comparative life cycle assessment of biomass utilization for electricity generation in the European Union and the United States. *Energy Policy*, 2019, 128, pp. 267-275. <https://doi.org/10.1016/j.enpol.2019.01.006>
- [30] Phanphanich, M.; Mani, S. Impact of torrefaction on the grindability and fuel characteristics of forest biomass. *Bioresour Technol*, 2011, 102 (2), pp. 1246-1253. <https://doi.org/10.1016/j.biortech.2010.08.028>
- [31] Lebaka, V. R. Potential bioresources as future sources of biofuels production: An overview. In: *Biofuel Technologies*, Gupta, V.; Tuohy, M. (eds.). Berlin: Springer; 2013, pp. 223-258. https://doi.org/10.1007/978-3-642-34519-7_9
- [32] Mesa, L. et al. Preliminary evaluation of organosolv pretreatment of sugar cane bagasse for glucose production: Application of 2³ experimental design. *Applied Energy*, 2010, 87 (1), pp. 109-114. <https://doi.org/10.1016/j.apenergy.2009.07.016>
- [33] Portha, J.-F. et al. Kinetics of methanol synthesis from carbon dioxide hydrogenation over copper-zinc oxide catalysts. *Industrial & Engineering Chemistry Research*, 2017, 56 (45), pp. 13133-13145. <https://doi.org/10.1021/acs.iecr.7b01323>

- [34] Government of India, Ministry of Power. Order on Biomass Co-firing. Accessed: July 10, 2025. Available at: <https://powermin.gov.in/sites/default/files/uploads/Orders/B.10.1.pdf>
- [35] Sasongko, N. A. et al. Biomass co-firing in coal power plants: Analyzing combustion characteristics and emission reductions. *Evergreen*, 2024, 11 (4), pp. 3576-3594. <https://doi.org/10.5109/7326991>
- [36] Ko, S.; Lautala, P. Optimal level of woody biomass co-firing with coal power plant considering advanced feedstock logistics system. *Agriculture*, 2018, 8 (6), 74. <https://doi.org/10.3390/agriculture8060074>
- [37] Sarkar, S. *Environmental assessment of biomass/torrefied biomass and waste coal co-fired power plants with the incorporation of carbon capture and storage technologies*. [master thesis], Georgia Southern University, Statesboro, GA, USA, 2024. Accessed: May 28, 2026. Available at: <https://digitalcommons.georgiasouthern.edu/etd/2874>
- [38] Government of India, Ministry of Power. SAMARTH – Sustainable Agrarian Mission on use of Agri-Residue in Thermal Power Plants. Accessed: July 10, 2025. Available at: <https://samarth.powermin.gov.in/>
- [39] Tumuluru, J. S.; Ghiasi, B.; Soelberg, N. R.; Sokhansanj, S. Biomass torrefaction process, product properties, reactor types, and moving bed reactor design concepts. *Frontiers in Energy Research*, 2021, 9, 728140. <https://doi.org/10.3389/fenrg.2021.728140>
- [40] Bello, R. S.; Olorunnisola, A. O.; Omoniyi, T. E.; Onilude, M. A. A review of technoeconomic benefits of torrefaction pretreatment technology and application in torrefying sawdust. *Sustaining Economies*, 2016, 2 (2), 104. <https://doi.org/10.62617/se.v2i2.104>
- [41] Devaraja, U. M. A.; Dissanayake, C. L. W.; Gunarathne, D. S.; Chen, W. H. Oxidative torrefaction and torrefaction-based biorefining of biomass: A critical review. *Biofuel Research Journal*, 2022, 9 (3), pp. 1672-1696. <https://doi.org/10.18331/BRJ2022.9.3.4>
- [42] Ahmad, R. et al. Influence of torrefaction on sewage sludge. *IOP Conference Series: Earth and Environmental Science*, 2023, 1135, 012036. <https://doi.org/10.1088/1755-1315/1135/1/012036>
- [43] Alizadeh, P. et al. Torrefaction and densification of wood sawdust for bioenergy applications. *Fuels*, 2022, 3 (1), pp. 152-175. <https://doi.org/10.3390/fuels3010010>
- [44] Kongto, P.; Palamanit, A.; Chaiprapat, S.; Tippayawong, N. Enhancing the fuel properties of rubberwood biomass by moving bed torrefaction process for further applications. *Renewable Energy*, 2021, 170, pp. 703-713. <https://doi.org/10.1016/j.renene.2021.02.012>
- [45] Guo, S. et al. An optimized method for evaluating the preparation of high-quality fuel from various types of biomasses through torrefaction. *Molecules*, 2024, 29 (8), 1889. <https://doi.org/10.3390/molecules29081889>
- [46] Hassan, I. et al. Impact of torrefaction process in elevating the fuel properties of selected herbaceous biomass solid waste. *Journal of Engineering Advancements*, 2024, 5 (03), pp. 64-70. <https://doi.org/10.38032/jea.2024.03.001>
- [47] Kanwal, S.; Chaudhry, N.; Munir, S.; Sana, H. Effect of torrefaction conditions on the physicochemical characterization of agricultural waste (sugarcane bagasse). *Waste Management*, 2019, 88, pp. 280-290. <https://doi.org/10.1016/j.wasman.2019.03.053>
- [48] Battista Jr, J. J.; Hughes, E. E.; Tillman, D. A. Biomass co-firing at Seward Station. *Biomass and Bioenergy*, 2000, 19 (6), pp. 419-427. [https://doi.org/10.1016/S0961-9534\(00\)00053-2](https://doi.org/10.1016/S0961-9534(00)00053-2)
- [49] Baxter, L. Biomass coal co-combustion: Opportunity for affordable renewable energy. *Fuel*, 2005, 84 (10), pp. 1295-1302. <https://doi.org/10.1016/j.fuel.2004.09.023>
- [50] Costello, R. Biomass co-firing offers cleaner future for coal plants. *Power Engineering*, 1999, 103 (1).

- [51] Mpungu, I. L. et al. Optimizing waste for energy: Exploring municipal solid waste variations on torrefaction and biochar production. *International Journal of Energy Research*, 2024, 2024 (1), 4311062. <https://doi.org/10.1155/2024/4311062>
- [52] Prayitno, H.; Lestari, R.; Kurniawansah, R. Potential torrefaction of tropical forest fruit waste. *Journal of Physics: Conference Series*, 2024, 2739, 012005. <https://doi.org/10.1088/1742-6596/2739/1/012005>
- [53] Chen, W. H. et al. Progress in biomass torrefaction: Principles, applications and challenges. *Progress in Energy and Combustion Science*, 2021, 82, 100887. <https://doi.org/10.1016/j.pecs.2020.100887>
- [54] Wang, S. et al. Effects of torrefaction on hemicellulose structural characteristics and pyrolysis behaviors. *Bioresource Technology*, 2016, 218, pp. 1106-1114. <https://doi.org/10.1016/j.biortech.2016.07.075>
- [55] Wulandari, W. et al. Heat transfer modelling of biomass torrefaction. *E3S Web of Conferences*, 2024, 543, 01002. <https://doi.org/10.1051/e3sconf/202454301002>
- [56] Voorspools, K.; Peersman, I.; D'haeseleer, W. A comparative analysis of energy and CO₂ taxes on the primary energy mix for electricity generation. *International Journal of Energy Research*, 2005, 29 (10), pp. 879-890. <https://doi.org/10.1002/er.1101>
- [57] Mignogna, D.; Szabó, M.; Ceci, P.; Avino, P. Biomass energy and biofuels: Perspective, potentials, and challenges in the energy transition. *Sustainability*, 2024, 16 (16), 7036. <https://doi.org/10.3390/su16167036>
- [58] Torres, C. M. M. E. et al. Torrefaction of kraft pulp mill sludges. *Scientific Reports*, 2023, 13, 22247. <https://doi.org/10.1038/s41598-023-46158-0>
- [59] Onyenwoke, C. et al. Effect of torrefaction on the physicochemical properties of white spruce sawdust for biofuel production. *Fuels*, 2023, 4 (1), pp. 111-131. <https://doi.org/10.3390/fuels4010008>
- [60] Banaget, C. K.; Check, G. R.; Watson, I. A. Torrefaction of plastics and food waste for biofuel production. *IOP Conference Series: Earth and Environmental Science*, 2023, 1201, 012009. <https://doi.org/10.1088/1755-1315/1201/1/012009>
- [61] ASTM International. ASTM D4442-16. *Standard Test Methods for Direct Moisture Content Measurement of Wood and Wood-Based Materials*. USA: ASTM; 2016. <https://doi.org/10.1520/D4442-16>
- [62] ASTM International. ASTM E1755-01. *Standard Test Method for Ash in Biomass*. USA: ASTM; 2015. <https://doi.org/10.1520/E1755-01R15>
- [63] ASTM International. ASTM E872-82. *Standard Test Method for Volatile Matter in the Analysis of Particulate Wood Fuels*. USA: ASTM; 2013. <https://doi.org/10.1520/E0872-82R19>
- [64] ASTM International. ASTM E711-87. *Standard Test Method for Gross Calorific Value of Refuse-Derived Fuel by the Bomb Calorimeter*. USA: ASTM; 2012. <https://doi.org/10.1520/E0711-23E01>
- [65] Zhang, C. et al. Oxidative torrefaction performance of microalga *Nannochloropsis oceanica* towards an upgraded microalgal solid biofuel. *Journal of Biotechnology*, 2021, 338, pp. 81-90. <https://doi.org/10.1016/j.jbiotec.2021.07.009>
- [66] Mei, Y. et al. Torrefaction of cedarwood in a pilot scale rotary kiln and the influence of industrial flue gas. *Bioresource Technology*, 2015, 177, pp. 355-360. <https://doi.org/10.1016/j.biortech.2014.10.113>
- [67] Liu, Y. et al. Torrefaction of corn straw in oxygen and carbon dioxide containing gases: Mass/energy yields and evolution of gaseous species. *Fuel*, 2021, 285, 119044. <https://doi.org/10.1016/j.fuel.2020.119044>
- [68] Fajobi, M. O. et al. Investigation of physicochemical characteristics of selected lignocellulosic biomass. *Scientific Reports*, 2022, 12 (1), 2918. <https://doi.org/10.1038/s41598-022-07061-2>
- [69] Ward, C. R.; Li, Z.; Gurba, L. W. Comparison of elemental composition of macerals determined by electron microprobe to whole-coal ultimate analysis data. *International*

- Journal of Coal Geology*, 2008, 75 (3), pp. 157-165. <https://doi.org/10.1016/j.coal.2008.05.010>
- [70] Rafey, A.; Pal, K.; Pant, K. K. Valorization of rice straw via torrefaction and its effect on the physicochemical properties. *Biomass Conversion and Biorefinery*, 2025, pp. 30423-30442. <https://doi.org/10.1007/s13399-024-06472-7>
- [71] Gajera, B.; Tyagi, U.; Sarma, A. K.; Jha, M. K. Impact of torrefaction on thermal behavior of wheat straw and groundnut stalk biomass: Kinetic and thermodynamic study. *Fuel Communications*, 2022, 12, 100073. <https://doi.org/10.1016/j.fueco.2022.100073>
- [72] Uemura, Y.; Omar, W. N.; Tsutsui, T.; Yusup, S. Torrefaction of oil palm wastes. *Fuel*, 2011, 90 (8), pp. 2585-2591. <https://doi.org/10.1016/j.fuel.2011.03.021>
- [73] Chen, W.-H.; Peng, J.; Bi, X. T. A state-of-the-art review of biomass torrefaction, densification and applications. *Renewable and Sustainable Energy Reviews*, 2015, 44, pp. 847-866. <https://doi.org/10.1016/j.rser.2014.12.039>
- [74] Deng, J. et al. Pretreatment of agricultural residues for co-gasification via torrefaction. *Journal of Analytical and Applied Pyrolysis*, 2009, 86 (2), pp. 331-337. <https://doi.org/10.1016/j.jaap.2009.08.006>
- [75] Chen, W.-H.; Kuo, P.-C. A study on torrefaction of various biomass materials and its impact on lignocellulosic structure simulated by thermogravimetry. *Energy*, 2010, 35 (6), pp. 2580-2586. <https://doi.org/10.1016/j.energy.2010.02.054>
- [76] Poudel, J.; Oh, S. C. Effect of torrefaction on the properties of corn stalk to enhance solid fuel qualities. *Energies*, 2014, 7 (9), pp. 5586-5600. <https://doi.org/10.3390/en7095586>